www.ietdl.org

Published in IET Signal Processing
Received on 19th November 2011
Revised on 26th September 2012
doi: 10.1049/iet-spr.2011.0430

ISSN 1751-9675

Sample-by-sample and block-adaptive robust constant modulus-based algorithms

A. Elnashar[1] S. Elnoubi[2] H. Elmikati[3]

[1]Wireless Broadband and Site Sharing, Network Development and Operation (ND&O), Technology, Emirates Integrated Telecom Company (EITC) 'du', P.O. Box 502666, Dubai, UAE
[2]Electrical Engineering Department, Alexandria University, Alexandria, Egypt
[3]Department of Communications and Electronics Engineering, Mansoura University, Mansoura, Egypt
E-mail: ayman.elnashar@du.ae

Abstract: In this study, a robust sample-by-sample linearly constrained constant modulus algorithm (LCCMA) and a robust adaptive block-Shanno constant modulus algorithm (BSCMA) are developed. The well-established quadratic inequality constraint approach is exploited to add robustness to the developed algorithms. The LCCMA algorithm is implemented using a fast steepest descent adaptive algorithm, whereas the BSCMA algorithm is realised using a modified Newton's algorithm without the inverse of Hessian matrix estimation. The developed algorithms are exercised to cancel the multiple access interference in a loaded direct sequence code division multiple access (DS/CDMA) system. Simulations are presented in a rich multipath environment with a severe near-far effect to evaluate the robustness of the proposed DS/CDMA detectors. Finally, a comprehensive comparative analysis between the sample-by-sample and block-adaptive constant modulus-based detectors is presented. It has been demonstrated that the developed robust BSCMA detector offers rapid convergence speed and very low computational complexity, whereas the developed robust LCCMA detector engenders about 5 dB improvement in the output signal-to-interference-plus-noise ratio over the BSCMA detector.

1 Introduction

It has been shown in [1] that the constant modulus algorithm (CMA) has a comparable performance to the training-based algorithms if undesirable local minima can be avoided. In [2], a near-far resistance initialisation procedure is proposed for the application of CMA to the uplink of the DS-CDMA system based on a pre-whitening for the received signal. Unfortunately, pre-whitening is an expensive operation to be implemented in an adaptive manner. In [3–5], a proper initialisation for the CMA is adopted to guarantee the desired source convergence. However, even with proper initialisation, there are conditions that must be met to guarantee global convergence. These conditions are based on the constant modulus (CM) cost function, Kurtosis and the signal-to-interference-plus-noise ratio (SINR). A linearly constrained CMA (LCCMA) is proposed in [6] to avoid the capture of an interference signal instead of the desired user. In the noise-free case, the proposed LCCMA in [6] can completely remove the multiple access interference (MAI), if, and only if, the desired user amplitude is not less than the critical value $1/\sqrt{3}$ [7]. Unfortunately, this is not a very realistic scenario in a practical DS/CDMA communication system because of the near-far effect and MAI. In [8,9], the constrained constant modulus (CCM) algorithm has been generalised to the multipath channels using multiple constraints. Moreover, a stochastic gradient algorithm is developed in [8] and a computationally efficient recursive least-squares algorithm is developed in [9]. It has been shown that the blind receiver design based on CCM criterion increased robustness against signature mismatch and provide improved performance over constrained minimum variance (CMV) algorithms [8, 9].

A modified version of the block Shanno's CMA (BSCMA) adaptive algorithm has been shown to offer a rapid convergence speed at low computational cost in [10–13]. However, the proposed BSCMA in [10–13] is notorious to suffer from sensitivity to the step-size selection and there is no clear strategy to update the step size. More importantly, the algorithm involves a gradient vector norm check and if the norm starts to increase, the algorithm stops the adaptive iteration and restates with the initial weight vector. Consequently, the subject block of data would not gain any benefit from the previous updates. Moreover, the BSCMA algorithm is sensitive to the number of iterations required for every block of data and there is no clear break point to stop the adaptive iteration within the block [10–13].

In addition to the LCCMA and BSCMA algorithms, a class of subspace or low-rank blind multiuser algorithms that can speed up the convergence, improve the tracking and are also robust against signature mismatch are developed in [14–16]. These algorithms employ eigenvalue-based subspace techniques [14], Krylov subspace methods [15], and an iterative approach for the construction of the subspace [16].

In this paper, we deploy the quadratic inequality (QI) constrained with the CCM criterion to improve the robustness of CM-based detectors [17–23]. The QI has been shown to improve the robustness of the CMV receivers against mismatch errors, uncertainties in estimating the data covariance matrix, random perturbations in detector parameters and the near-far effect [18]. We first develop a robust LCCMA formulation and then its sample-by-sample adaptive realisation is derived [17]. The developed robust LCCMA detector is implemented using a fast steepest descent adaptive algorithm based on the partition linear interference canceller (PLIC) structure [18] with multiple constraints and a QI constraint [17–19] on the adaptive portion of the PLIC structure. The Lagrange multiplier method is used to solve the quadratic constraint [18–21]. The developed LCCMA detector offers the highest performance and the best robustness among the existing CM-based algorithms. However, the proposed robust LCCMA detector with the QI constraint requires high computational load compared to the classical CM-based algorithms.

Secondly, a robust BSCMA detector with low complexity is developed in order to enhance the performance of the traditional BSCMA algorithm [23]. The QI constraint oversees the weight vector norm and consequently controls the gradient vector norm, and hence there is no need to verify the gradient vector norm during block-adaptive iteration. In addition, the iteration within the block may continue to a predetermined fixed number of iterations without affecting the algorithm stability because of the mentioned reason. The different forms of the BSCMA algorithms, the block-conjugate gradient CMA (BCGCMA) algorithm and the block-gradient descent CMA (BGDCMA) algorithm, are developed and analysed in the same context.

The developed sample-by-sample and block-adaptive CM-based algorithms are exploited to update the adaptive portion of the PLIC structure. The developed algorithms are used to identify and mitigate the MAI in a loaded DS/CDMA system and hence avoid interference capture as in the traditional CM-based algorithms. Finally, a comparative analysis is conducted between the developed sample-by-sample and block-adaptive DS/CDMA detectors in terms of performance, computational complexity and convergence speed. It is demonstrated that the robust BSCMA detector offers rapid convergence speed and the lowest computational complexity, whereas the robust LCCMA detector engenders about 5 dB improvement in the output SINR over the robust BSCMA detector.

The rest of the paper is organised as follows. The realisation of the sample-by-sample LCCMA detector is provided in Section 2. The robust BSCMA detector is developed in Section 3. The detailed comparative analysis is presented in Section 4. Finally, conclusions are summarised in Section 5.

2 Robust-adaptive sample-by-sample LCCMA detector

In a DS/CDMA system, we can generally impose a set of linear constraints to avoid the cancellation of the interested signal scattered in different multipath during minimisation of the dispersion of the receiver output (i.e. CM cost function). The constraints are of the form $\boldsymbol{C}_1^{\mathrm{H}}\boldsymbol{f} = \boldsymbol{g}$ where $\boldsymbol{C}_1$ is an $N \times K$ matrix consisting of shifted versions of the interested user signature waveform, $\boldsymbol{g}$ is a $K \times 1$ constraint vector and $\boldsymbol{f}$ is the $N \times 1$ detector vector.

Consequently, the so-called LCCMA detector can be obtained by solving the following code-constrained minimisation problem [6–9]

$$\min_{\boldsymbol{f}} J_1(\boldsymbol{f}) \triangleq E\{(|\boldsymbol{f}^{\mathrm{H}}\boldsymbol{x}|^2 - r)^2\} \quad \text{s.t.} \quad \boldsymbol{C}_1^{H}\boldsymbol{f} = \boldsymbol{g} \tag{1}$$

where r is a constant.

An alternative formulation for the LCCMA can be realised as follows [24]

$$\min_{\boldsymbol{f}} J_2(\boldsymbol{f}) \triangleq E\{(\boldsymbol{f}^{\mathrm{H}}\bar{\boldsymbol{x}} - r)^2\} \quad \text{s.t.} \quad \boldsymbol{C}_1^{\mathrm{H}}\boldsymbol{f} = \boldsymbol{g} \tag{2}$$

where $\bar{\boldsymbol{x}}(i) = \boldsymbol{x}(i)y(i)$. The cost function in (2) can be reformulated as follows

$$J_2(\boldsymbol{f}) \triangleq -\boldsymbol{f}^{\mathrm{H}}E\{r\bar{\boldsymbol{x}}\} + \boldsymbol{f}^{\mathrm{H}}E\{\bar{\boldsymbol{x}}\bar{\boldsymbol{x}}^{\mathrm{H}}\}\boldsymbol{f} \tag{3}$$

As a result, we obtain

$$J_2(\boldsymbol{f}) \triangleq -\boldsymbol{f}^{\mathrm{H}}\boldsymbol{\omega}(n) + \boldsymbol{f}^{\mathrm{H}}\boldsymbol{\Pi}(n)\boldsymbol{f} \tag{4}$$

where $\boldsymbol{\omega}(n) = E\{r\bar{\boldsymbol{x}}\}$ and $\boldsymbol{\Pi}(n) = E\{\bar{\boldsymbol{x}}\bar{\boldsymbol{x}}^{H}\}$ denote, respectively, a new cross-correlation vector and a modified autocorrelation matrix. Fortunately, the proposed cost function in (4) is analogous to the minimum output energy (MOE) detector cost function (i.e. $\boldsymbol{f}^{\mathrm{H}}\boldsymbol{R}(n)\boldsymbol{f}$) where $\boldsymbol{R}(n)$ is the autocorrelation matrix (i.e. $E\{\boldsymbol{x}\boldsymbol{x}^{\mathrm{H}}\}$). Therefore the robust LCCMA detector can be derived similar to the developed robust MOE detector in [18].

According to the above discussion, the PLIC structure [18, 19] is adopted with the CM-based cost functions in (1) and (4). In addition, the quadratic constraint is applied on the adaptive weight portion (i.e. $\boldsymbol{f}_{\mathrm{a}}$) of $\boldsymbol{f} = \boldsymbol{f}_{\mathrm{c}} - \boldsymbol{B}\boldsymbol{f}_{\mathrm{a}}$, where $\boldsymbol{f}_{\mathrm{c}}$ is an $(N \times 1)$ non-adapting vector satisfying the constraints (i.e. $\boldsymbol{C}_1^{H}\boldsymbol{f} = \boldsymbol{g}$), $\boldsymbol{f}_{\mathrm{a}}$ is $(L \times 1,\ L = N - K)$ vector, which can be updated without constraints and $\boldsymbol{B}$ is an $N \times L$ blocking matrix inserted to ensure the orthogonality between upper and lower branches of the PLIC structure. Therefore the optimal robust weight vector corresponding to (1) and (4) can be obtained, respectively, from the solution of the following constrained optimisation problems

$$\min_{\boldsymbol{f}_{\mathrm{a}}} J_1(\boldsymbol{f}_{\mathrm{a}}) \triangleq E\{(|(\boldsymbol{f}_{\mathrm{c}} - \boldsymbol{B}\boldsymbol{f}_{\mathrm{a}})^{\mathrm{H}}\boldsymbol{x}|^2 - r)^2\} \quad \text{s.t.} \quad \boldsymbol{f}_{\mathrm{a}}^{\mathrm{H}}\boldsymbol{f}_{\mathrm{a}} \le \beta^2 \tag{5}$$

$$\min_{\boldsymbol{f}_{\mathrm{a}}} J_2(\boldsymbol{f}_{\mathrm{a}}) \triangleq -(\boldsymbol{f}_{\mathrm{c}} - \boldsymbol{B}\boldsymbol{f}_{\mathrm{a}})^{\mathrm{H}}\boldsymbol{\omega}(n) + (\boldsymbol{f}_{\mathrm{c}} - \boldsymbol{B}\boldsymbol{f}_{\mathrm{a}})^{\mathrm{H}}\boldsymbol{\Pi}(n)(\boldsymbol{f}_{\mathrm{c}} - \boldsymbol{B}\boldsymbol{f}_{\mathrm{a}}) \quad \text{s.t.} \quad \boldsymbol{f}_{\mathrm{a}}^{\mathrm{H}}\boldsymbol{f}_{\mathrm{a}} \le \beta^2 \tag{6}$$

where β is the constrained value, which satisfies $\beta^2 = \rho^2 - \boldsymbol{f}_{\mathrm{c}}^{\mathrm{H}}\boldsymbol{f}_{\mathrm{c}}$ and $\rho^2 = t.(||\boldsymbol{f}_{\mathrm{c}}||^2)$. The constant t should be set to a suitable value as demonstrated in Subsection 4.1.

By considering the optimisation problem given in (6), the constrained optimisation problem in (5) can be derived in a manner similar to (6). Owing to similarity, we will only examine the associated detector in the performance comparison Section 4.1), the method of Lagrangian multipliers [17, 18] is exploited to solve it by forming the

doi: 10.1049/iet-spr.2011.0430

following Lagrangian function

$$J_2(\boldsymbol{f}_a) = -(\boldsymbol{f}_c - \boldsymbol{B}\boldsymbol{f}_a)^H\boldsymbol{\omega}(n) + (\boldsymbol{f}_c - \boldsymbol{B}\boldsymbol{f}_a)^H\boldsymbol{\Pi}(n)(\boldsymbol{f}_c - \boldsymbol{B}\boldsymbol{f}_a) + \frac{1}{2}\lambda t(\boldsymbol{f}_a^H\boldsymbol{f}_a - \beta^2) \tag{7}$$

The optimal solution of (7) is obtained by taking the gradient of $J_2(\boldsymbol{f}_a)$ with respect to $\boldsymbol{f}_a^H$ and then setting the resulting quantities to zero, we obtain

$$\boldsymbol{f}_{a(opt)} = (\boldsymbol{\Pi}_{\boldsymbol{B}} + \lambda\boldsymbol{I})^{-1}(\boldsymbol{p}_{\boldsymbol{B}} - \boldsymbol{B}^H\boldsymbol{\omega}) \tag{8}$$

where

$$\boldsymbol{\Pi}_{\boldsymbol{B}} = \boldsymbol{B}^H\boldsymbol{\Pi}\boldsymbol{B},\ \boldsymbol{p}_{\boldsymbol{B}} = \boldsymbol{P}_{\boldsymbol{B}}\boldsymbol{f}_c \text{ and } \boldsymbol{P}_{\boldsymbol{B}} = \boldsymbol{B}^H\boldsymbol{\Pi}$$

Similar to the approach proposed in [18], a variable loading (VL) technique, which is capable of precisely computing the optimal diagonal loading term λ, is developed. The steepest descent method is used to adaptively update the optimum weight vector that minimises the Lagrangian function in (7) and consequently

$$\boldsymbol{f}_a(n) = \boldsymbol{f}_a(n-1) - \mu\nabla J_2(\boldsymbol{f}_a) \tag{9}$$

where μ is the step size of the algorithm and $\nabla J_2(\boldsymbol{f}_a)$ is the conjugate derivative of $J_2(\boldsymbol{f}_a)$ with respect to $\boldsymbol{f}_a^H(n)$ and is given by

$$\nabla J_2(\boldsymbol{f}_a) \Rightarrow \boldsymbol{\tau}(n) = \boldsymbol{B}^H\boldsymbol{\omega}(n) - \boldsymbol{B}^H\boldsymbol{\Pi}(n)\boldsymbol{f}_c + \boldsymbol{B}^H\boldsymbol{\Pi}(n)\boldsymbol{B}\boldsymbol{f}_a(n-1) + \lambda\boldsymbol{f}_a(n-1) \tag{10}$$

Therefore the adaptive implementation of $\boldsymbol{f}_a(n)$ can be obtained by substituting (10) into (9) as follows

$$\boldsymbol{f}_a(n) = \boldsymbol{f}_a(n-1) - \mu(\boldsymbol{B}^H\boldsymbol{\omega}(n) + \boldsymbol{\Pi}_{\boldsymbol{B}}(n)\boldsymbol{f}_a(n-1) - \boldsymbol{p}_{\boldsymbol{B}}(n)) - \mu\lambda\boldsymbol{f}_a(n-1) \tag{11}$$

Since the QI constraint $\boldsymbol{f}_a^H(n)\boldsymbol{f}_a(n) \le \beta^2$ should be satisfied at each iteration step, and by substituting from (9) and assuming that the QI constraint is satisfied in the previous step, we obtain

$$(\bar{\boldsymbol{f}}_a(n) - \mu\lambda\boldsymbol{f}_a(n-1))^H(\bar{\boldsymbol{f}}_a(n) - \mu\lambda\boldsymbol{f}_a(n-1)) \le \beta^2 \tag{12}$$

$$\bar{\boldsymbol{f}}_a(n) = \boldsymbol{f}_a(n-1) - \mu\bar{\boldsymbol{\tau}}(n) \tag{13}$$

where

$$\bar{\boldsymbol{\tau}}(n) = \boldsymbol{B}^H\boldsymbol{\omega}(n) + \boldsymbol{\Pi}_{\boldsymbol{B}}(n)\boldsymbol{f}_a(n-1) - \boldsymbol{p}_{\boldsymbol{B}}(n) \tag{14}$$

The value of λ can be found by solving the following quadratic equation

$$\mu(n)^2\boldsymbol{f}_a^H(n-1)\boldsymbol{f}_a(n-1)\lambda^2 - 2\mu(n)\bar{\boldsymbol{f}}_a^H(n)\boldsymbol{f}_a(n-1)\lambda + \bar{\boldsymbol{f}}_a^H(n)\bar{\boldsymbol{f}}_a(n) - \beta^2 = 0 \tag{15}$$

Therefore the optimal diagonal loading term λ which satisfies the inequality constraint is

$$\lambda(n) = \frac{b \pm \sqrt{b^2 - 4ac}}{2a} \tag{16}$$

where

$$a = \mu(n)^2||\boldsymbol{f}_a(n-1)||^2,$$
$$b = 2\mu(n)\bar{\boldsymbol{f}}_a^H(n)\boldsymbol{f}_a(n-1), \text{ and } c = \bar{\boldsymbol{f}}_a^H(n)\bar{\boldsymbol{f}}_a(n) - \beta^2 \tag{17}$$

A sample-by-sample adaptive implementation for the proposed robust-adaptive detector can be realised using the VL technique as shown in Fig. 1.

3 Robust block-adaptive BSCMA detector

In this section, a robust block-adaptive BSCMA detector is realised similar to the early-developed robust LCCMA detector. We first extend the CM cost function in (1) to admit block processing similar to the approach in [10–13]. If we take a block from the received vector signal with length $N \times M$, where M is the block length (i.e. number of data bits), thus

$$D_i = [\boldsymbol{x}((i-1)M) \vdots \boldsymbol{x}((i-1)M+1) \vdots \cdots \vdots \boldsymbol{x}(iM-1)] \in R^{N\times M} \tag{18}$$

The block CM objective function is defined as

$$\Psi(\boldsymbol{f}) = \frac{1}{4M}\sum_{l=0}^{M-1}[|\boldsymbol{f}^H\boldsymbol{x}((i-1)M+l)|^2 - 1]^2 \tag{19}$$

where i refers to the block index and $0 \le l < M$ refers to iteration index within the block. The length of the $\boldsymbol{x}[(i-1)M+l]$ equals to the detector length, that is, N.

The objective function is modified to satisfy the real requirement of Shanno's algorithm as follows:

$$\Psi(\boldsymbol{f}) = \frac{1}{4M}\sum_{n=0}^{M-1}[\boldsymbol{f}^H\boldsymbol{X}(n)\boldsymbol{f} - l]^2 \tag{20}$$

and

$$\nabla\Psi(\boldsymbol{f}) = \frac{1}{M}\sum_{n=0}^{M-1}[\boldsymbol{f}^H\boldsymbol{X}(n)\boldsymbol{f} - 1]\boldsymbol{X}(n)\boldsymbol{f} \tag{21}$$

where $\boldsymbol{X}(n) = \boldsymbol{x}^H(n)\boldsymbol{x}(n)$ for real data samples and we can adopt the approach proposed in [11] to convert it from complex values to real values as follows

$$\boldsymbol{f}(n) = \begin{bmatrix}\text{Re}\{\boldsymbol{f}(n)\}\\ \text{Im}\{\boldsymbol{f}(n)\}\end{bmatrix} \tag{22}$$

$$\boldsymbol{X}(n) = \boldsymbol{x}_f(n)\boldsymbol{x}_f^T(n) + \boldsymbol{x}_b(n)\boldsymbol{x}_b^T(n) \tag{23}$$

where

$$\boldsymbol{x}_f(n) = \begin{bmatrix}\text{Re}\{\boldsymbol{x}(n)\}\\ -\text{Im}\{\boldsymbol{x}(n)\}\end{bmatrix},\quad \boldsymbol{x}_b(n) = \begin{bmatrix}\text{Re}\{\boldsymbol{x}(n)\}\\ -\text{Im}\{\boldsymbol{x}(n)\}\end{bmatrix} \tag{24}$$

- *Initialisation:*
    - $\boldsymbol{\Pi}_B(0) = B^{\mathrm{H}}(\boldsymbol{I}_L)\boldsymbol{B}$; $\boldsymbol{f}_c = \boldsymbol{C}_1\left(C_1^{\mathrm{H}}\,\boldsymbol{C}_1\right)^{-1}\boldsymbol{g}$; $\boldsymbol{I}_L$ is $L \times L$ identity matrix.
    - $\rho^2 = t.\left(\|\boldsymbol{f}_c\|^2\right), \beta^2 = \rho^2 - \|\boldsymbol{f}_c\|^2$, $\boldsymbol{f}_a(0) = 0_L^{\mathrm{T}}$; $\boldsymbol{0}_L$ is $L \times 1$ zero vector.
    - $\lambda(0) = 0$; $\bar{\boldsymbol{\tau}}(0) = B^{\mathrm{H}}\,(\boldsymbol{I}_L)\,\boldsymbol{f}_c$; $\eta = 1$
- *For* $n = 1, 2, \cdots$, *do*
    - $\boldsymbol{z}(n) = B^{\mathrm{H}}\,\boldsymbol{x}(n)$; $4LN$
    - $y(n) = x^{\mathrm{H}}\,(n)\boldsymbol{f}_c + z^{\mathrm{H}}\,(n)\boldsymbol{f}_{\mathrm{a}}(n-1)$; $2N + 2L$
    - $\bar{\boldsymbol{z}}(n) = y(n)\boldsymbol{z}(n)$
    - $e(n) = 1 - |y(n)|^2$
    - $\boldsymbol{\Pi}_B(n) = \eta\,\boldsymbol{\Pi}_B(n-1) + \bar{\boldsymbol{z}}^H(n)\bar{\boldsymbol{z}}(n)$; $4L$
    - $\boldsymbol{\tau}(n-1) = \bar{\boldsymbol{\tau}}(n-1) + \lambda(n-1)\,\boldsymbol{f}_{\mathrm{a}}(n-1)$
    - $\bar{\boldsymbol{\tau}}(n) = \eta\,\bar{\boldsymbol{\tau}}(n-1) - e(n)\bar{\boldsymbol{z}}(n) - \mu(n-1)\boldsymbol{\Pi}_B(n)\boldsymbol{\tau}(n-1)$, $4L^2$, see [18] and [25]
    - $\mu(n) = \dfrac{\gamma\boldsymbol{\tau}^{\mathrm{H}}(n-1)\boldsymbol{\tau}(n-1)}{\boldsymbol{\tau}^{\mathrm{H}}(n-1)\boldsymbol{\Pi}_B(n)\boldsymbol{\tau}(n-1)}$; $3L$;
    - $\bar{\boldsymbol{f}}_{\mathrm{a}}(n) = \boldsymbol{f}_{\mathrm{a}}(n-1) - \mu_{\mathrm{opt}}(n)\bar{\boldsymbol{\tau}}(n)$

    - *If* $\left\|\bar{\boldsymbol{f}}_{\mathrm{a}}(n)\right\|^2 > \beta^2$;check step for quadratic constraint
        - $c = \bar{\boldsymbol{f}}_a^{\mathrm{H}}(n)\bar{\boldsymbol{f}}_{\mathrm{a}}(n) - \beta^2$, L
        - $b = -2\mu\bar{\boldsymbol{f}}_{\mathrm{a}}^{H}(n)\boldsymbol{f}_{\mathrm{a}}(n-1)$, $2L$
        - $a = \mu(n)^2\,\|\boldsymbol{f}_{\mathrm{a}}(n-1)\|^2$; L
        - $\lambda(n) = \dfrac{-b - \left(\sqrt{b^2 - 4ac}\right)}{2a}$
        - $\boldsymbol{f}_a(n) = \bar{\boldsymbol{f}}_{\mathrm{a}}(n) - \mu_{\mathrm{opt}}(n)\lambda(n)\,\boldsymbol{f}_{\mathrm{a}}(n-1)$
    - *else*;
        - $\boldsymbol{f}_{\mathrm{a}}(n) = \bar{\boldsymbol{f}}_{\mathrm{a}}(n)$
        - $\lambda(n) = 0$
    - *End if*
- *End for*

End

Fig. 1 *Summary of the robust adaptive sample-by-sample LCCMA detector*

The well-known Newton's algorithm is used to update the adaptive portion of the PLIC structure as follows

$$\boldsymbol{f}_{\mathrm{a}}(j) = \boldsymbol{f}_{\mathrm{a}}(j-1) - \boldsymbol{H}^{-1}(\boldsymbol{f}_{\mathrm{a}}(j-1))\boldsymbol{g}(\boldsymbol{f}_{\mathrm{a}}(j-1)) \qquad (25)$$

where $\boldsymbol{H}^{-1}(\boldsymbol{f}_{\mathrm{a}}(j-1))$ is the Hessian of the objective function $\Psi(\boldsymbol{f})$ and $\boldsymbol{g}[\boldsymbol{f}_{\mathrm{a}}(j-1)]$ is the gradient of the cost function with respect to $\boldsymbol{f}_{\mathrm{a}}$ evaluated at the iteration index $j-1$, where j is the iteration index within the block of data. Shanno's approximation is used to approximate the inverse of Hessian's matrix with $O(M)$ complexity. Shanno's approximation matrix is implicitly determined by the gradients of the two most recent iterations, a search direction and a step size based on the previous iteration as follows

$$\boldsymbol{H}_{\mathrm{Newton}}^{-1}(\boldsymbol{f}_{\mathrm{a}}(j-1)) = \boldsymbol{I} - \frac{\boldsymbol{u}(j)\boldsymbol{d}^{\mathrm{T}}(j-1) - \boldsymbol{d}^{\mathrm{T}}(j-1)[c(j)\boldsymbol{d}^{\mathrm{T}}(j-1) - \boldsymbol{u}^{\mathrm{T}}(j)]}{\boldsymbol{d}^{\mathrm{T}}(j-1)\boldsymbol{u}(j)} \qquad (26)$$

where

$$c(j) = \delta(j-1) + \frac{|\boldsymbol{u}(j)|^2}{\boldsymbol{d}^{\mathrm{T}}(j-1)\boldsymbol{u}(j)} \qquad (27)$$

$$\boldsymbol{u}(j) = \boldsymbol{g}(\boldsymbol{f}_{\mathrm{a}}(j)) - \boldsymbol{g}(\boldsymbol{f}_{\mathrm{a}}(j-1)) \qquad (28)$$

$$\boldsymbol{d}(j) = -\boldsymbol{H}^{-1}(\boldsymbol{f}_{\mathrm{a}}(j-1))\boldsymbol{g}(\boldsymbol{f}_{\mathrm{a}}(j-1)) \qquad (29)$$

The step size is $\delta(j-1)$ and hence the adaptive weight vector can be updated as follows

$$\boldsymbol{f}_{\mathrm{a}}(j) = \boldsymbol{f}_{\mathrm{a}}(j-1) + \delta(j)\boldsymbol{d}(j) \qquad (30)$$

To guarantee the convergence, the step size should satisfy the following constraints [10–13]

$$\Psi(\boldsymbol{f}_{\mathrm{a}}(j-1) + \delta(j)\boldsymbol{d}(j)) \leq \Psi(\boldsymbol{f}_{\mathrm{a}}(j-1)) + \alpha\delta(j)\boldsymbol{g}^{\mathrm{T}}(\boldsymbol{f}_{\mathrm{a}}(j-1))\boldsymbol{d}(j) \qquad (31)$$

$$(\boldsymbol{g}(\boldsymbol{f}_{\mathrm{a}}(j)))^{\mathrm{T}}\boldsymbol{d}(j) \geq \sigma(\boldsymbol{g}(\boldsymbol{f}_{\mathrm{a}}(j-1)))^{\mathrm{T}}\boldsymbol{d}(j) \qquad (32)$$

IET Signal Process., 2012, Vol. 6, Iss. 8, pp. 805–813
doi: 10.1049/iet-spr.2011.0430

A procedure for selecting the step size according to the above constraints is outlined in [10] and [12].

Substituting (27), (28) into (26) and then substituting into (29) and after some manipulations, the following updated equation for $\boldsymbol{d}(j)$ can be obtained

$$\boldsymbol{d}(j) = \boldsymbol{d}(j-1)e(j) + (a(j)-1)\boldsymbol{g}(\boldsymbol{f}_{\mathrm{a}}(j-1)) \tag{33}$$

where

$$a(j) = \frac{\boldsymbol{u}(j)\boldsymbol{d}^{\mathrm{T}}(j-1)}{\boldsymbol{d}^{\mathrm{T}}(j-1)\boldsymbol{u}(j)} \tag{34}$$

and

$$e(j) = \frac{[\boldsymbol{u}^{\mathrm{T}}(j) - c(j)\boldsymbol{d}^{\mathrm{T}}(j-1)]\boldsymbol{g}(\boldsymbol{f}_{\mathrm{a}}(j-1))}{\boldsymbol{d}^{\mathrm{T}}(j-1)\boldsymbol{u}(j)} \tag{35}$$

If we set $a(j) = 0$, we obtain the BCGCMA algorithm (The robust versions of the BCGCMA and BGDCMA algorithms can be straightforward derived similar to the robust BSCMA detector. Owing to the similarity, we will only analyse the associated detectors in the performance comparison Section 4.1), and if we set $a(j) = e(j) = 0$, we obtain the BGDCMA algorithm [10, 11, 23].

The quadratic constraint can be applied on the adaptive weight portion that is, $\boldsymbol{f}_{\mathrm{a}}(j)$. Consequently, the robust weight vector can be obtained from the solution of the following constrained optimisation problem [23]

$$\hat{\Psi}(\hat{\boldsymbol{f}}_{\mathrm{a}}) = \frac{1}{4M}\sum_{n=0}^{M-1}[\hat{\boldsymbol{f}}_{\mathrm{a}}^{\mathrm{T}}(j)\boldsymbol{Z}(n)\hat{\boldsymbol{f}}_{\mathrm{a}}(j) - 1]^2$$
$$\text{subject to } \hat{\boldsymbol{f}}_{\mathrm{a}}^{\mathrm{H}}(j)\hat{\boldsymbol{f}}_{\mathrm{a}}(j) \leq \beta^2 \tag{36}$$

where '^' stands for the quadratically constrained detector.

Unfortunately, there is no closed-form solution for the above optimisation problem similar to the LCCMA detector. Alternatively, the BSCMA is invoked to update the detector and the Lagrangian methodology is used to solve the QI constraint. The new cost function and the gradient vector are formed, respectively, as follows

$$\hat{\Psi}(\hat{\boldsymbol{f}}_{\mathrm{a}}) = \frac{1}{4M}\sum_{n=0}^{M-1}[\hat{\boldsymbol{f}}_{\mathrm{a}}^{\mathrm{H}}(j)\boldsymbol{Z}(n)\hat{\boldsymbol{f}}_{\mathrm{a}}(j) - 1]^2 + \frac{1}{2}\zeta s(\hat{\boldsymbol{f}}_{\mathrm{a}}^{\mathrm{T}}(j)\hat{\boldsymbol{f}}_{\mathrm{a}}(j) - \beta^2) \tag{37}$$

$$\hat{\boldsymbol{g}}(\hat{\boldsymbol{f}}_{\mathrm{a}}(j-1)) = \frac{1}{M}\sum_{n=0}^{M-1}[\hat{\boldsymbol{f}}_{\mathrm{a}}^{\mathrm{T}}(j-1)\boldsymbol{Z}(n)\hat{\boldsymbol{f}}_{\mathrm{a}}(j-1) - 1]\boldsymbol{Z}(n)\hat{\boldsymbol{f}}_{\mathrm{a}}(j-1) + \zeta(j)\hat{\boldsymbol{f}}_{\mathrm{a}}(j-1) \tag{38}$$

Therefore

$$\hat{\boldsymbol{d}}(j) = -\boldsymbol{H}^{-1}(\hat{\boldsymbol{f}}_{\mathrm{a}}(j-1))[\boldsymbol{g}(\hat{\boldsymbol{f}}_{\mathrm{a}}(j-1)) + \zeta(j)\hat{\boldsymbol{f}}_{\mathrm{a}}(j-1)] \tag{39}$$

In order to simplify the computation of the Lagrange multiplier $\zeta(j)$ and to avoid the computation of the Hessian matrix, the QI term in (37) is updated using the steepest descent algorithm rather than Newton's algorithm and, consequently, we obtain

$$\hat{\boldsymbol{d}}(j) = -\boldsymbol{H}^{-1}(\hat{\boldsymbol{f}}_{\mathrm{a}}(j-1))\boldsymbol{g}(\hat{\boldsymbol{f}}_{\mathrm{a}}(j-1)) + \zeta(j)\hat{\boldsymbol{f}}_{\mathrm{a}}(j-1) \tag{40}$$

then

$$\hat{\boldsymbol{f}}_{\mathrm{a}}(j) = \hat{\boldsymbol{f}}_{\mathrm{a}}(j-1) - \delta(j)\boldsymbol{H}^{-1}(\hat{\boldsymbol{f}}_{\mathrm{a}}(j-1))\boldsymbol{g}(\hat{\boldsymbol{f}}_{\mathrm{a}}(j-1)) + \delta(j)\zeta(j)\hat{\boldsymbol{f}}_{\mathrm{a}}(j-1) \tag{41}$$

$$\hat{\boldsymbol{f}}_{\mathrm{a}}(j) = \boldsymbol{f}_{\mathrm{a}}(j) + \delta(j)\zeta(j)\hat{\boldsymbol{f}}_{\mathrm{a}}(j-1) \tag{42}$$

where

$$\boldsymbol{f}_{\mathrm{a}}(j) = \bar{\boldsymbol{f}}_{\mathrm{a}}(j-1) - \delta(j)\boldsymbol{H}^{-1}(\bar{\boldsymbol{f}}_{\mathrm{a}}(j-1))\boldsymbol{g}(\bar{\boldsymbol{f}}_{\mathrm{a}}(j-1)) \tag{43}$$

Using the update of $\hat{\boldsymbol{f}}_{\mathrm{a}}(j)$ in (42) into the constraint $\hat{\boldsymbol{f}}_{\mathrm{a}}^{H}(j)\hat{\boldsymbol{f}}_{\mathrm{a}}(j) \leq \beta^2$, the constrained value $\zeta(j)$ can be obtained as follows [23]

$$\zeta(j) = \left[\bar{b} \pm \sqrt{\bar{b}^2 - 4\overline{ac}}\right]/2\bar{a} \tag{44}$$

where

$$\bar{a} = \delta^2(j)||\hat{\boldsymbol{f}}_{\mathrm{a}}(j-1)||^2 \tag{45}$$

$$\bar{b} = 2\delta(j)\boldsymbol{f}_{\mathrm{a}}^{\mathrm{T}}(j)\hat{\boldsymbol{f}}_{\mathrm{a}}(j-1) \tag{46}$$

$$\bar{c} = ||\boldsymbol{f}_{\mathrm{a}}(j)||^2 - \beta^2 \tag{47}$$

By substituting (45)–(47) and (43) into $b^2 - 4ac \geq 0$, the following inequality is obtained

$$[(\hat{\boldsymbol{f}}_{\mathrm{a}}(j-1) + \delta(j)\boldsymbol{d}(j))^{\mathrm{T}}\hat{\boldsymbol{f}}_{\mathrm{a}}(j-1)]^2 \geq ||\hat{\boldsymbol{f}}_{\mathrm{a}}(j-1)||^2[(\hat{\boldsymbol{f}}_{\mathrm{a}}(j-1) + \delta(j)\boldsymbol{d}(j))^{\mathrm{T}}(\hat{\boldsymbol{f}}_{\mathrm{a}}(j-1) + \delta(j)\boldsymbol{d}(j)) - \beta^2] \tag{48}$$

After some manipulations to (48), the following upper-bound inequality on the step size is obtained [18, 23]

$$\delta(j) \leq \frac{\beta||\hat{\boldsymbol{f}}_{\mathrm{a}}(j-1)||}{\sqrt{||\hat{\boldsymbol{f}}_{\mathrm{a}}(j-1)||^2||\boldsymbol{d}(j)||^2 - \boldsymbol{d}^{\mathrm{T}}(j)\hat{\boldsymbol{f}}_{\mathrm{a}}(j-1)\hat{\boldsymbol{f}}_{\mathrm{a}}^{\mathrm{T}}(j-1)\boldsymbol{d}(j)}} \tag{49}$$

Therefore this upper-bound inequality constraint guarantees real positive roots in (44) and consequently the optimal loading level can be attained. In addition, the two constraints in (31) and (32) must be considered as well to guarantee the convergence of the BSCMA algorithm.

The proposed robust BSCMA detector based on block Shanno's algorithm and the VL technique along with multiplication complexity is summarised in Fig. 2. There are two main loops in the algorithm. The outer loop is for each block of data and the inner loop is repeated over the same block of data till certain number of iterations is completed. It is worth mentioning that there is no need to apply an upper-bound constraint on the gradient vector norm similar to the legacy BSCMA algorithm since the quadratic constraint on $\boldsymbol{f}_{\mathrm{a}}$ oversees and manages the gradient vector norm increase. A block of data with length $N \times M$ is selected and the output of the lower branch of the PLIC structure $\boldsymbol{z}(n)$ is computed. The adaptive vector $\hat{\boldsymbol{f}}_{\mathrm{a}}(1, 1)$ is initialised with the signature sequence of the interested user. On the other hand, the final weight vector $\hat{\boldsymbol{f}}_{\mathrm{a}}(i, j)$ of each block is used as an initial vector to the next

- Initialisation:
  - $\rho^2 = t.\left(\|\boldsymbol{f}_c\|^2\right), \beta^2 = \rho^2 - \|\boldsymbol{f}_c\|^2, \varepsilon = 0.1$
  - $\zeta(0) = 0\,;\boldsymbol{d}(0) = \boldsymbol{g}\left(f_a(0)\right), \alpha = 0.25,\ \sigma = 0.5$
- For $i = 1, 2, \cdots, \lceil N/M \rceil$ *outer loop on block basis*
  - $D_i = \left[\boldsymbol{x}((i-1)M) \vdots \boldsymbol{x}((i-1)M+1) \vdots \cdots \vdots \boldsymbol{x}(iM-1)\right]$
    - if $(i=1)$ $\hat{f}_a(1,1) = \boldsymbol{B}^T c_1$, c_1 *is the signature of the interested user.*
    - Else $\hat{f}_a(i,1) = \hat{f}_a(i,j)$; *initialise* $\bar{\boldsymbol{f}}_a$ *with the last updated value of the previous block.*
  - $j = 0$
  - For $j = 1, 2, \cdots,$ *until converge or max number of iterations reach*
  - $\boldsymbol{Z}(n) = z(n)z^T(n)$ $4L$, where $z(n) = \boldsymbol{B}^T\boldsymbol{x}(n)$; $4LN$
    - $\bar{g}\left(\hat{f}_a(i,j-1)\right) = \frac{1}{M}\sum_{n=0}^{M-1}\left[\hat{f}_a^{\,T}(i,j-1)\boldsymbol{Z}(n)\hat{f}_a(i,j-1) - 1\right]\boldsymbol{Z}(n)\hat{\boldsymbol{f}}(i,j-1)_a - \lambda(j-1)\hat{\boldsymbol{f}}_a(i,j-1)$; $6LM$
    - If $\boldsymbol{j} = \boldsymbol{1}$
      - $\boldsymbol{d}(j) = \hat{\boldsymbol{g}}\left(\hat{f}_a(i,j-1)\right)$
    - Else
      - $\boldsymbol{d}(j) = \boldsymbol{d}(j-1)e(j) + \left(a(j)-1\right)\hat{\boldsymbol{g}}\left(\hat{f}_a(i,j-1)\right)$; $6L$ *are required for (34) & (35)*
    - $f_a(i,j) = \hat{f}_a(i,j-1) + \delta(j)\boldsymbol{d}(j)$
    - *if* $\left(\|f_a(i,j)\|^2 > \beta^2\right)$;
      - $c = \|f_a(i,j)\|^2 - \beta^2$, L
      - $b = 2\delta(j)\,\boldsymbol{f}_a^T(i,j)\,\hat{\boldsymbol{f}}_a(i,j-1)$, $2L$
      - $a = \delta^2(j)\left\|\hat{\boldsymbol{f}}_a(i,j-1)\right\|^2$, L
      - $\zeta(j) = \left[b \pm \sqrt{b^2 - 4ac}\right]/2a$
      - $\hat{\boldsymbol{f}}_a(i,j) = f_a(i,j) + \zeta(j)\delta(j)\hat{\boldsymbol{f}}_a(i,j-1)$
    - *else*
      - $\hat{\boldsymbol{f}}_a(i,j) = f_a(i,j)$; $\zeta(j) = 0$
    - End if
    - If $\left[\Phi\left(\hat{\boldsymbol{f}}_a(i,j)\right) \le \Phi\left(\hat{\boldsymbol{f}}_a(i,j-1)\right) + \alpha\delta(j)\left(\hat{\boldsymbol{g}}\left(\hat{\boldsymbol{f}}_a(i,j-1)\right)\right)^T\hat{\boldsymbol{d}}(j)\right]$; $2L$
      - $\delta(j+1) = \delta(j) + \varepsilon\delta(j)$
    - *Else if* $\left[\left(\hat{\boldsymbol{g}}\left(\hat{\boldsymbol{f}}_a(j)\right)\right)^T\hat{\boldsymbol{d}}(j) \ge \sigma\left(\hat{\boldsymbol{g}}\left(\hat{\boldsymbol{f}}_a(j-1)\right)\right)^T\hat{\boldsymbol{d}}(j)\right]$; $2L$
      - $\delta(j+1) = \delta(j) - \varepsilon\delta(j)$
    - *Else if*
      - $\delta(j) > \frac{\beta\left\|\hat{\boldsymbol{f}}_a(j-1)\right\|}{\sqrt{\left\|\hat{\boldsymbol{f}}_a(j-1)\right\|^2\|\boldsymbol{d}(j)\|^2 - \boldsymbol{d}^T(j)\hat{\boldsymbol{f}}_a(j-1)\hat{\boldsymbol{f}}_a^T(j-1)\boldsymbol{d}(j)}} = \delta(j+1)$; $3L$
    - *Otherwise*
      - $\delta(j+1) = \delta(j)$
    - *End if*
  - *End of j loop*
- $\boldsymbol{f}(i,j) = \boldsymbol{f}_c - \boldsymbol{B}\hat{\boldsymbol{f}}_a(i,j)$; *for evaluation only.*
- $\boldsymbol{y}\left(((i-1)M):(iM-1)\right) = \boldsymbol{x}\left(((i-1)M):(iM-1)\right)\boldsymbol{f}(i,j)$
- *End for i loop*

Fig. 2 *Summary of the robust block-adaptive BSCMA detector*

doi: 10.1049/iet-spr.2011.0430

block (i.e.$\hat{\boldsymbol{f}}_a(i+1,1)=\hat{\boldsymbol{f}}_a(i,j)$). The gradient vector is estimated considering the previous diagonal loading term $\lambda(j-1)\hat{\boldsymbol{f}}_a(i,j-1)$, to avoid computing it with $\hat{\boldsymbol{d}}(j)$, which requires Hessian matrix computation as shown in (39). The vector $\boldsymbol{d}(j)$ is computed according to (33) and then the initial adaptive vector is updated using (30).

If the norm constraint on $\boldsymbol{f}_a(i,j)$ is not met, the VL technique is invoked to fulfil the QI constraint. Unfortunately, there is no closed form for the optimum step size, since the cost function in (37) is not a quadratic function and hence there is no global minimum for it as a function of the step size. Alternatively, a new procedure based on the approach in [10] along with upper bound in (49) is developed as shown in Fig. 2 to estimate the step size. After convergence of a certain bock of data, the output of this block is computed.

4 Comparative analysis

4.1 Performance comparison

Five synchronous users in a multipath Rayleigh-fading channel with five multipath components are simulated. Gold codes are used. The code length is 31 chips and the detector length is assumed to be one bit length (i.e. $N = 31$). The channel length (max delay spread) is assumed to be ten delayed components and multipath delays are randomly distributed. The detector is assumed to be synchronised to the required user. Users are assumed to have equal power except for the required user is assumed to be 10 dB less than other users to simulate a severe near–far effect scenario. Two performance meters are adopted; the output SINR and bit-error rate (BER) against bit/block iterations for sample-by-sample and block-adaptive algorithms, respectively.

4.1.1 Robust-adaptive sample-by-sample LCCMA detector: In this section, the performance of the proposed robust-adaptive sample-by-sample LCCMA detector is investigated and compared with different CM-based detectors. The detectors designed based on the cost functions in (1) and (6) are referred to them, respectively, as LCCMA1 and LCCMA2. Three LCCMA1-based detectors are simulated as follows; LCCMA1 without weighting, LCCMA1 with de-biased weighting [2] and LCCMA1 with weighting and with QI constraint on the weight vector norm. The three LCCMA1-based detectors are referred to as, LCCMA1 w/t W., LCCMA1 w. W. and LCCMA1 w. VL, respectively. The VL technique is used with the LCCMA1 w. VL detector to achieve the QI constraint. Straightforward steps are required, similar to the detector in Fig. 1, to compute the diagonal loading term

Table 1 Initialisation parameters for the sample-by-sample CM-based detectors

Detector	T	Robust technique	γ
LCCMA1 w/t W.	—	—	0.1
LCCMA1 w. W.	—	—	0.1
LCCMA1 w. VL	1.6	VL	0.1
LCCMA2 w/t QI	—	—	0.9
LCCMA2 w. SP	1.3	SP	0.001
LCCMA2 w. VL	1.3	VL	0.001
LCCMA2 w. CG	—	—	0.9

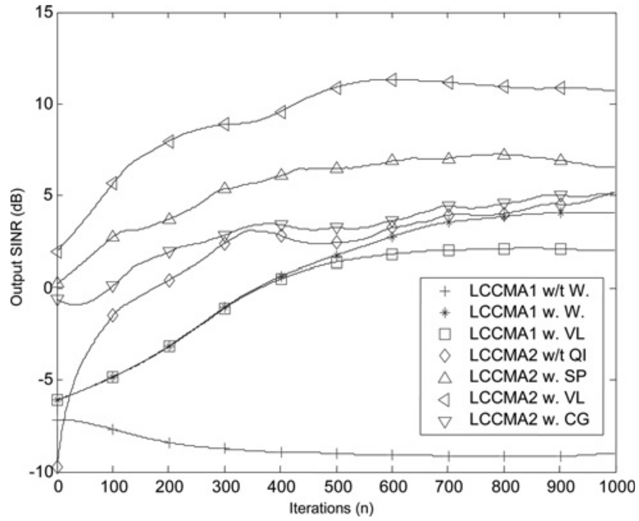

Fig. 3 *SINR against bit iterations for the sample-by-sample LCCMA-based adaptive detectors*

and the LCCMA1 w. VL detector based on the cost function in (1). The LCCMA1-based detectors are adapted using the well-known stochastic gradient algorithm. The LCCMA2 cost function is used to develop three detectors. The first detector does not include the QI constraint, the second detector is with the scaled projection (SP) technique, developed in [26], to satisfy the QI constraint and the third detector is with the proposed VL technique as shown in Fig. 1. In addition, an LCCMA2-based detector with the conjugate gradient algorithm addressed in [24, 25] is simulated as well. The four detectors are referred to as, LCCMA2 w/t QI, LCCMA2 w. SP, LCCMA2 w. VL and LCCMA2 w. CG, respectively. The initialisations of the seven simulated detectors are summarised in Table 1. The selection of the constant t in Table 1 is based on a compromise between robustness and performance optimality and it is estimated empirically from multiple simulation runs.

Figs. 3 and 4 show the SINR and BER, respectively, for the seven detectors against bit iteration. The BER behaviour of the different CM-based detectors is well presented by their SINR performance, but is not mapped exactly. For example, the LCCMA2 w/t QI detector has initial degradation in

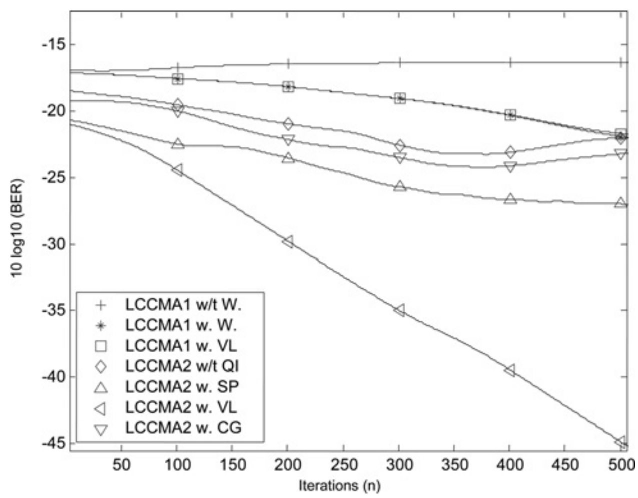

Fig. 4 *BER against bit iterations for the sample-by-sample LCCMA-based adaptive detectors*

SINR performance, whereas its BER performance is not impacted upon by this initial degradation. It is concluded from these figures that combining the QI constraint with the LCCMA2-based detectors substantially improves their performance and robustness against the near-far effect compared to their peers without the QI constraint. More importantly, the proposed VL technique deployed with LCCMA2 w. VL detector significantly outperforms the SP technique deployed with LCCMA2 w. SP detector. Furthermore, the QI constraint does not appear to offer any performance improvement for the LCCMA1-based detectors. In addition to this, weighting is a mandatory initialisation technique to guarantee global convergence of the LCCMA1-based detectors. More specifically, the global convergence of the LCCMA1-based detectors can be guaranteed, if and only if, $a_1 \geq 1/\sqrt{3}$ [7] where a_1 is the amplitude of the desired user. Finally, the LCCMA2 w. CG has a little performance improvement over the LCCMA2 w/t QI detector.

4.1.2 Robust block-adaptive BSCMA detector: In this section, the performance of the BSCMA detector and its two subsidiaries (i.e. BCGCMA and BGDCMA) are compared with the developed robust detectors. The three robust detectors are referred to as BSCMA w. VL, BCGCMA w. VL and BGDCMA w. VL, respectively.

The block data length is 100 bits and the number of iterations inside the block is 25 iterations. The performance of the six detectors is assessed in terms of output SINR and BER against block iterations. Figs. 5 and 6 show the SINR and BER for the six detectors, respectively. These figures demonstrate that the QI constraint offers considerable improvement for the BSCMA detector and its variants (i.e. BCGCMA and BGDCMA). The convergence of the robust detectors are attained after about 100 block iterations which means that four blocks of data are required for convergence. On the other hand, the non-robust detectors require about 150 block iterations for convergence. In addition, the steady-state behaviour of the robust detectors supersedes the corresponding non-robust detectors.

It is interesting now to compare the performance of the robust LCCMA-based detectors with that of the robust BSCMA-based detectors. The LCCMA2 w. VL detector outperforms the BSCMA w. VL detector in terms of steady-state performance. More specifically, the LCCMA2 w. VL detector offers about 5 dB improvement in SINR. However, the BSCMA w. VL engenders rapid convergence speed, as the BSCMA w. VL requires almost 100 iterations to converge, whereas the LCCMA2 w. VL requires at least 550 iterations to converge. As a final observation, the QI constraint adds significant improvement to the LCCMA2-based detectors compared to the BSCMA-based detectors.

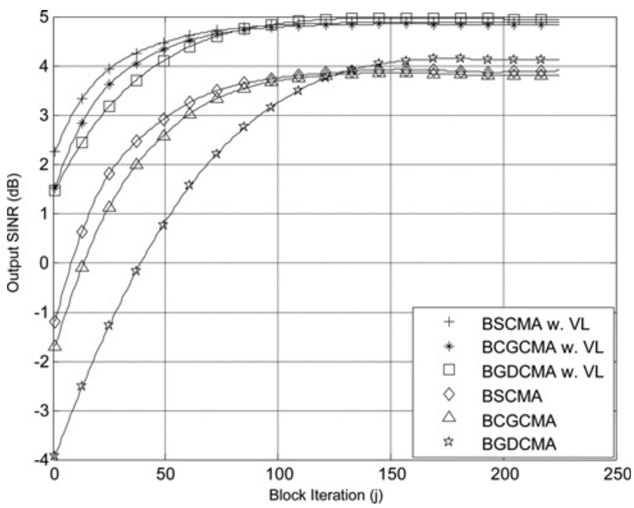

Fig. 5 *SINR against block iterations for the block-adaptive BSCMA-based detectors*

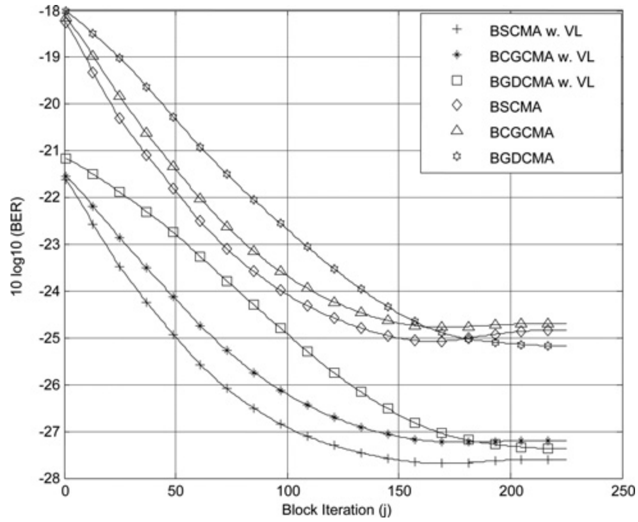

Fig. 6 *BER against block iterations for the block-adaptive BSCMA-based detectors*

4.2 Complexity analysis

The required amount of multiplications at each iteration step of the robust-adaptive detector LCCMA2 w. VL is provided in Fig. 1. Therefore the total amount of the required multiplications for each sample of the proposed LCCMA2 w. VL detector during adaptive implementation is about $O(4L^2 + 4LN + 13L + 2N)$.

On the other side, and as illustrated in Fig. 2, the multiplication complexity of the proposed robust BSCMA w. VL detector is about $O(17L + 6LM)$ per output point from every block of data with length M. Then, the maximum multiplication complexity per block is $O[(17L + 6LM)J]$ assuming that the maximum number of iterations is always attained, where J is the maximum

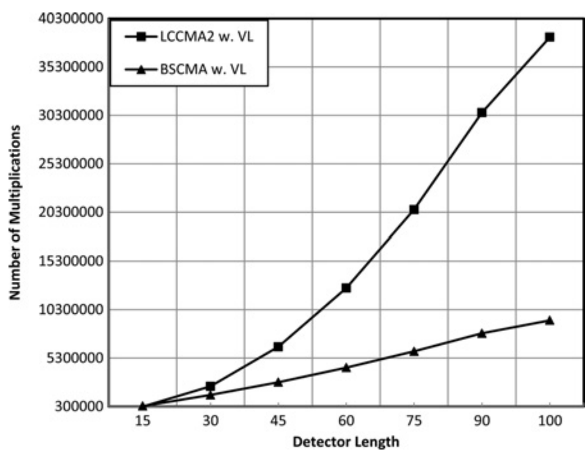

Fig. 7 *Computational complexity of the developed robust detectors against detector length*

IET Signal Process., 2012, Vol. 6, Iss. 8, pp. 805–813
doi: 10.1049/iet-spr.2011.0430

number of iterations within the block and therefore the total multiplication complexity till convergence is $O[(21L + 6LM + 4LN)JI]$, where I is the number of blocks required for convergence.

As demonstrated in Section 4.1, four blocks are required for convergence of the robust BSCMA w. VL detector and the number of iterations inside the block is 25 iterations. Therefore the maximum multiplication complexities required for convergence of the BSCMA w. VL is about $[(21L + 6LM + 4LN)100]$, whereas the LCCMA2 w. VL detector requires about $[(4L^2 + 4LN + 13L + 2N)550]$ till convergence. By considering the simulation scenario in Section 4.1 with $L = 21$, $N = 31$ and $M = 100$ bits, the robust BSCMA detector requires about 1 564 500 multiplications, whereas the LCCMA2 w. VL detector requires about 2 586 650 multiplications that is, $O(4L^2 + 4LN + 13L + 2N)|_{L=21, N=31}$. Therefore the robust BSCMA w. VL detector offers significant complexity reduction compared to the robust LCCMA2 w. VL. Furthermore, the multiplication complexity against the detector length (i.e. N) for the two detectors has been demonstrated in Fig. 7. It is concluded from this figure that the BSCAM w. VL detector offers very low computational complexity compared to the LCCMA w. VL detector and it is evident that the complexity of the BSCMA w. VL detector increases almost linearly with the detector length, whereas the complexity of LCCMA w. VL detector increases exponentially with the detector length.

5 Conclusions

The contribution in this paper is three-fold. First, we developed a robust sample-by-sample adaptive detector based on the LCCMA algorithm and the QI constraint. The simulations results demonstrated that the proposed robust LCCMA detector (i.e. LCCMA2 w. VL) outperforms other CM-based detectors in terms of robustness and steady-state performance. More specifically, the detector is robust against the near-far effect and the amplitude restriction on the interested user recovery is no longer mandatory for the global convergence of the algorithm. Secondly, we developed a new robust block-adaptive detector based on the BSCMA algorithm and the QI constraint. The simulations results demonstrated that the new proposed detector outperforms the standard BSCMA algorithm in both robustness and steady-state performance. Finally, a detailed comparative analysis between the proposed robust detectors is conducted in terms of performance and complexity analysis. More specifically, the robust LCCMA2 w. VL detector offers 5 dB improvement in the output SINR over the robust BSCMA w. VL detector, whereas the latter offers faster convergence speed and very low computational complexity.

6 References

1 Zeng, H.H., Tong, L., Johnson, Jr., C.R.: 'Relationships between the constant modulus and Wiener receivers', *IEEE Trans. Inf. Theory*, 1998, **44**, pp. 1523–1538

2 Schniter, P., Johnson, Jr., C.R.: 'Minimum-entropy blind acquisition/equalization for uplink DS-CDMA'. Proc. 36th Allerton Conf. Comm., Control and Computing, 1998

3 Schniter, P., Johnson, Jr., C.R.: 'Sufficient conditions for the local convergence of constant modulus algorithms', *IEEE Trans. Signal Process.*, 2000 [see also *IEEE Trans. on Acoust. Speech Signal Process.*], **48**, pp. 2785–2796

4 Lopez-Valcarce, R., Perez-Gonzalez, F.: 'Efficient reinitialization of the prewhitened constant modulus algorithm', *IEEE Commun. Lett.*, 2001, **5**, (12), pp. 488–490

5 Evans, S., Tong, L.: 'Online adaptive reinitialization of constant modulus algorithm', *IEEE Trans. Commun.*, 2000, **48**, pp. 537–539

6 Miguez, J., Castedo, L.: 'A linearly constrained constant modulus approach to blind adaptive multiuser interference suppression', *IEEE Commun. Lett.*, 1998, **2**, (8), pp. 217–219

7 Jiang, H., Kwak, K.S.: 'A non-canonical linearly constrained constant modulus algorithm for a blind multiuser detector', *ETRI J.*, 2002, **24**, (3), pp. 239–246

8 Xu, Z., Liu, P.: 'Code-constrained blind detection of CDMA signals in multipath channels', *IEEE Signal Process. Lett.*, 2002, **9**, (12), pp. 389–392

9 de Lamare, R.C., Sampaio Neto, R.: 'Blind adaptive code-constrained constant modulus algorithms for CDMA interference suppression in multipath channels', *IEEE Commun. Lett.*, 2005, **9**, (4)

10 Wang, Z., Dowling, E.M.: 'Block-Shanno constant modulus algorithm for wireless equalizations'. Proc. ICASSP, Atlanta, GA, USA, April 1996, pp. 2678–2681

11 Jani, U.G., Dowling, E.M., Golden, R.M., Wang, Z.: 'Multiuser interference suppression using block Shanno constant modulus algorithm', *IEEE Trans. Signal Process.*, 2000, **48**, (5), pp. 334–336

12 Samir, T., Elnoubi, S., Elnashar, A.: 'Block-Shanno minimum BER beamforming', *IEEE Trans. Veh. Technol.*, 2008, **57**, (5), pp. 2981–2990

13 Paik, D., Torlak, M., Dowling, E.M.: 'Blind adaptive CDMA processing for smart antennas using the block shanno constant modulus algorithm', *IEEE Trans. Signal Process.*, 2005, **54**, (5), pp. 1956–1959

14 Dong, E., Zhu, C., Evans, L.: 'Blind multiuser detector based on reduced rank subspace and least square constant modulus algorithm'. Eighth Int. Conf. Signal Processing, 2006

15 de Lamare, R.C., Haardt, M., Sampaio-Neto, R.: 'Blind adaptive constrained reduced-rank parameter estimation based on constant modulus design for CDMA interference suppression', *IEEE Trans. Signal Process.*, 2008, **56**, (6), pp. 2470–2482

16 de Lamare, R.C., Sampaio-Neto, R., Haardt, M.: 'Blind adaptive constrained constant-modulus reduced-rank interference suppression algorithms based on interpolation and switched decimation', *IEEE Trans. Signal Process.*, 2011, **59**, (2), pp. 681–695

17 Elnashar, A., Elnoubi, S., Elmikati, H.: 'A robust linearly constrained CMA for adaptive blind multiuser detection'. Proc. IEEE WCNC 2005 Conf., New Orleans, LA, USA, 13–17 March 2005, vol. 1, pp. 233–238

18 Elnashar, A., Elnoubi, S., Elmikati, H.: 'Low-complexity robust adaptive generalized sidelobe canceller detector for DS/CDMA systems', *Int. J. Adapt. Control Signal Process.*, 2008, **23**, (3), pp. 293–310

19 Elnashar, A.: 'On efficient implementation of robust adaptive beamforming based on worst-case performance optimization', *IET Signal Process.*, 2008, **2**, (4), pp. 381–393

20 Elnashar, A., Elnoubi, S., Elmikati, H.: 'Performance analysis of blind adaptive MOE multiuser receivers using inverse QRD-RLS algorithm', *IEEE Trans. Circuits Syst. I*, 2008, **55**, (1), pp. 398–411

21 Elnashar, A., Elnoubi, S., Elmikati, H.: 'Further study on robust adaptive beamforming with optimum diagonal loading', *IEEE Trans. Antennas Propag.*, 2006, **54**, (12), pp. 3647–3658

22 Schodorf, J.B., Williams, D.B.: 'A constrained optimization approach to multi-user detection', *IEEE Trans. Signal Process.*, 1997, **45**, (1), pp. 258–262

23 Elnashar, A., Elnoubi, S., Elmikati, H.: 'A robust block-shanno adaptive blind multiuser receiver for DS-CDMA systems'. Proc. IST Mobile and Wireless Communications Summit 2005, Dresden, Germany, June 2005, 19–23

24 Chern, S.-J., Wang, S.-M.: 'Adaptive multiuser detector for DS-CDMA over multipath fading channel with linearly constrained constant modulus modified conjugate gradient algorithm'. ISPACS 2003, December 2003, vol. A3-3, pp. 301–307

25 Chang, P.S., Willson, Jr., A.N.: 'Analysis of conjugate gradient algorithms for adaptive filtering', *IEEE Trans. Signal Process.*, 2000, **48**, (2), pp. 409–418

26 Cox, H., Zeskind, R., Qwen, M.: 'Robust adaptive beamforming', *IEEE Trans. Acoust. Speech Signal Process.*, 1987, **ASSP-35**, (10), pp. 1365–1376